THE JOURNAL OF BIOLOGICAL CHEMISTRY VOL. 285, NO. 45, pp. 34699–34707, November 5, 2010
© 2010 by The American Society for Biochemistry and Molecular Biology, Inc. Printed in the U.S.A.

K_v7-type Channel Currents in Spiral Ganglion Neurons

INVOLVEMENT IN SENSORINEURAL HEARING LOSS[*S]

Received for publication, April 20, 2010, and in revised form, August 24, 2010 Published, JBC Papers in Press, August 25, 2010, DOI 10.1074/jbc.M110.136192

Ping Lv, Dongguang Wei, and Ebenezer N. Yamoah[1]

From the Department of Anesthesiology and Pain Medicine, Program in Communication Science, School of Medicine, University of California, Davis, California 95618

Alterations in K_v7-mediated currents in excitable cells result in several diseased conditions. A case in DFNA2, an autosomal dominant version of progressive hearing loss, involves degeneration of hair cells and spiral ganglion neurons (SGNs) from basal to apical cochlea, manifesting as high-to-low frequency hearing loss, and has been ascribed to mutations in $K_v7.4$ channels. Analyses of the cellular mechanisms of $K_v7.4$ mutations and progressive degeneration of SGNs have been hampered by the paucity of functional data on the role K_v7 channels play in young and adult neurons. To understand the cellular mechanisms of the disease in SGNs, we examined temporal (young, 0.5 months old, and senescent, 17 months old) and spatial (apical and basal) roles of K_v7-mediated currents. We report that differential contribution of K_v7 currents in mice SGNs results in distinct and profound variations of the membrane properties of basal *versus* apical neurons. The current produces a major impact on the resting membrane potential of basal neurons. Inhibition of the current promotes membrane depolarization, resulting in activation of Ca^{2+} currents and a sustained rise in intracellular Ca^{2+}. Using TUNEL assay, we demonstrate that a sustained increase in intracellular Ca^{2+} mediated by inhibition of K_v7 current results in significant SGN apoptotic death. Thus, this study provides evidence of the cellular etiology and mechanisms of SGN degeneration in DFNA2.

Mutations in K_v7 (KCNQ) channels are associated with several pathological conditions ranging from epileptic seizures in $K_v7.2/3$ (1, 2), deafness as seen in Jervell and Lange Nielsen syndrome in $K_v7.1$ (3), and an autosomal dominant form of nonsyndromic hearing loss, which usually progresses from high-to-low frequencies (progressive high frequency hearing loss, DFNA2) in $K_v7.4$ (4, 5). Although none of the underlying cellular and molecular mechanisms of the K_v7-associated clinical syndromes are fully understood, the etiology of $K_v7.4$-mediated hearing loss is the least appreciated, and the progressive nature of the disease makes it most insidious. Several previous studies have targeted hair cells as the site of the disease mechanism (4–6), but others have invoked the involvement of dysfunctional cochlear nucleus afferent signal transmission (4). Also predicted is the disruption of K^+ recirculation in the cochlear duct (7). Moreover, these recognized mechanisms are derived mainly from the expression pattern of $K_v7.4$ at the peripheral and central auditory pathways (7). $K_v7.4$ channels have been reported in vestibular hair cells (4, 8), but there are no reported imbalance symptoms in subjects carrying $K_v7.4$ mutations (5), suggesting that the auditory deficit ensues from distinct cell-specific functional roles of the channel.

In DFNA2, there is a spatiotemporal course in deterioration of hair cells. Outer hair cells in the basal cochlea are affected first, shortly after the onset of hearing, followed by the apical turn (4, 6, 7, 9). Degeneration of outer hair cells is presumably followed by inner hair cells (IHCs)[2] and then loss of spiral ganglion neurons (SGNs) (4, 6, 7). Although there are clear examples of hearing loss associated with primary degeneration of SGNs (10, 11), it has been asserted in several forms of hearing loss that loss of SGNs occurs secondary to hair cell loss, because release of trophic factors from hair cells unto SGNs is necessary for their survival (12, 13). Perhaps most puzzlingly is why degeneration of hair cells apparently precedes SGNs because they also express $K_v7.4$ and K_v7 channel subtypes (7, 14). Because K_v7 channels are activated at low membrane voltages (approximately −80 mV), they contribute substantially in establishing the resting membrane voltage (V_{rest}) of IHCs and, in doing so, control intracellular Ca^{2+} concentration (15, 16). To determine the roles of K_v7 channel currents in SGNs and to identify the potential cellular mechanisms for $K_v7.4$ mutation-associated degeneration of these neurons, we surmised that in DFNA2 loss of SGNs may occur independent of hair cell loss.

In this study, we demonstrate that linopirdine- and retigabine-sensitive currents produce a major impact on the V_{rest} and membrane excitability of young, adult, and senescent mouse SGNs. Moreover, differential expression of the current at apex-to-base axis of the cochlea and during aging may produce alterations in intracellular Ca^{2+} concentration, resulting in Ca^{2+}-mediated apoptotic cell death. We conclude that in DFNA2 the loss of SGNs may occur independently and/or simultaneously with hair cell loss.

EXPERIMENTAL PROCEDURES

Isolation of Postnatal and Adult SGNs—This investigation was performed in accordance with the guidelines of the Animal Care and Use Committee of the University of California, Davis.

* This work was supported, in whole or in part, by National Institutes of Health Grant DC010386 (to E. N. Y.).

[S] The on-line version of this article (available at http://www.jbc.org) contains supplemental Fig. S1 and Tables S1–S8.

[1] To whom correspondence should be addressed: Dept. of Anesthesiology and Pain Medicine, Program in Communication Science, University of California, 1515 Newton Ct., Davis, CA 95618. Tel.: 530-754-6630; Fax: 530-754-7183; E-mail: enyamoah@ucdavis.edu.

[2] The abbreviations used are: IHC, inner hair cell; SGN, spiral ganglion neuron; BDNF, brain-derived neurotrophic factor; NT3, neurotrophin-3; AP, action potential.

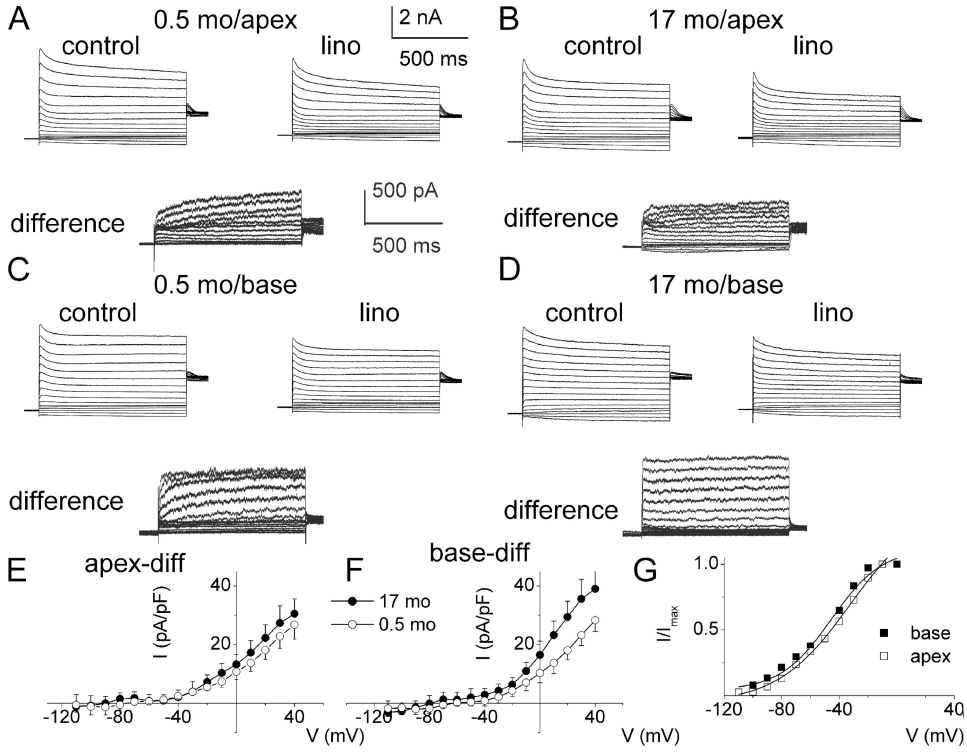

FIGURE 1. **Whole-cell K^+ currents recorded from young and old SGNs of mice.** *A*, representative traces from SGNs from the apex of the cochlea, a family of K^+ currents obtained from a holding potential of −90 mV and stepped up from −100 to +40 mV, with $\Delta V = 10$ mV. The tail currents were obtained at −40 mV. The *left* and *right panels* show control traces from 2-week-old (0.5-month-old (*0.5 mo*)) neurons from the apical aspects of the cochlea and traces after application of 10 μM linopirdine (*lino*), respectively. The *panel below* (labeled "*difference*") illustrates the difference-current traces, which represent the linopirdine-sensitive current. Similar data were obtained using bepridil (data not shown). Inward Na^+ and Ca^{2+} currents were removed by substituting choline for sodium and calcium ions. *B*, data obtained from old SGNs isolated from the apical portion of 17-month-old (*17-mo*) mice. Control traces, traces after application of 10 μM linopirdine, and the linopirdine-sensitive current traces are shown as described for *A*. *C*, similar data obtained from SGNs at the base of the cochlea from 0.5-month-old mice, showing control (*left panel*) after application of linopirdine (*right panel*) and linopirdine-sensitive current traces *below* (*difference*). *D*, current traces recorded from 17-month-old SGNs from basal neurons (*left panel*) and the resulting traces after application of linopirdine (10 μM) and the drug-sensitive current (shown below). *E* and *F*, current density-voltage curve obtained from apical (*E*) and basal (*F*) SGNs (mean ± S.D., $n = 11$ neurons). *diff*, difference. *G*, activation curves of tail currents of basal neurons (■) had $V_{1/2} = -48 \pm 3$ mV and slope factor, *k*, of 18 ± 4 mV ($n = 17$) compared with apical neurons (□) with $V_{1/2} = -45 \pm 5$ mV and $k = 20 \pm 3$ mV ($n = 16$). Moreover, the voltage-dependent properties ($V_{1/2}$ and *k*, in mV) of the linopirdine-sensitive currents for apical SGNs of 0.5, 3–4, and 17 months old were −43 ± 4 and 19 ± 4 ($n = 11$), −41 ± 5 and 18 ± 4 ($n = 12$), and −42 ± 4 and 20 ± 2 ($n = 9$), respectively. For basal SGNs at 0.5, 3–4, and 17 months old, the $V_{1/2}$ and *k*, in mV values, were −44 ± 4, 17 ± 4 ($n = 14$), −45 ± 4, 18 ± 3 ($n = 15$), and −46 ± 5, 18 ± 4 ($n = 10$), respectively.

Isolation of SGNs followed the detailed procedure outlined in a previous study (17). To ensure that adequate and satisfactory electrophysiological experiments were performed, we cultured SGNs for ~24–48 h to allow the detachment of Schwann cells from the surfaces of the neurons. C57BL/6J mice were sacrificed, and the temporal bones were removed in solution containing minimum essential medium with Hanks' salt (Invitrogen) and 0.2 g/liter kynurenic acid, 10 mM $MgCl_2$, 2% FBS (fetal bovine serum; v/v), and glucose (6 g/liter). The central spiral ganglion tissue was dissected out and split into apical and basal pieces across the modiolar axis. The tissue was digested in an enzyme mixture containing collagenase type I (1 mg/ml) and DNase (1 mg/ml) at 37 °C for 20 min. After a series of gentle trituration and centrifugation in 0.45 M sucrose, the cell pellets were reconstituted in 900 ml of culture media (Neurobasal™ A, supplemented with 2% B27 (v/v), 0.5 mM L-glutamine, 100 units/ml penicillin; Invitrogen) and filtered through a 40-μm cell strainer for cell culture and electrophysiological experiments. We pooled three 2-week-old postnatal and 3–4- and 17-month-old mice into each SGN culture. SGNs were kept in culture for ~24–48 h to allow Schwann cells to detach from the cell bodies. Electrophysiological experiments were performed at room temperature (21–23 °C). All reagents were obtained from Sigma, unless otherwise specified.

Electrophysiology—Whole-cell voltage clamp recordings of K^+ currents in SGNs were performed using an Axopatch 200B amplifier (Molecular Devices, Sunnyvale, CA). Fire-polished electrodes (3–5 megohms) were pulled from borosilicate glass. The electrodes contained (in mM) the following: KCl 140, $MgCl_2$ 1, HEPES 10, EGTA 5, $CaCl_2$ 1, K_2ATP 4, pH 7.2, with KOH. The external bath solution was constantly perfused (~2–3 ml/min) and contained (in mM) the following: NaCl or choline-Cl 145, KCl 2, $CaCl_2$ 1.8, $MgCl_2$ 0.5, HEPES 10, D-glucose 5, pH 7.4, with NaOH. Outward K^+ current traces were generated with depolarizing voltage steps from a holding potential of −90 mV and stepped to varying positive potentials ($\Delta V = 10$ mV). Currents were measured with capacitance and series resistance compensations (>90%), filtered at 2 kHz using an 8-pole Bessel filter, and sampled at 5 kHz. Whole-cell K^+ current amplitudes at varying test potentials were measured at the peak and steady-state levels using a peak and steady-state detection routine; the current was divided by the cell capacitance (picofarads) to generate the current density-voltage relationship. The K_v7-mediated currents were assessed as linopirdine- and/or retigabine-sensitive currents. The capacitative transients were used to estimate cell capacitance as an indirect measure of cell size. The seal resistance was typically 5–20 gigaohms. The liquid junction potentials were measured and corrected.

Action potentials were amplified (100 times), filtered (bandpass 2–10 kHz), and digitized at 5–50 kHz using the Digidata 1200 (Molecular Devices) as described earlier (18, 19). Extracellular solution for most experiments contained (in mM) the following: NaCl 145, KCl 2, $MgCl_2$ 0.5, $CaCl_2$ 1.8, D-glucose 5, HEPES 10, pH 7.4. The stock solutions of all channel blockers and activators used were made either in double distilled H_2O or DMSO and stored at −20 °C. The

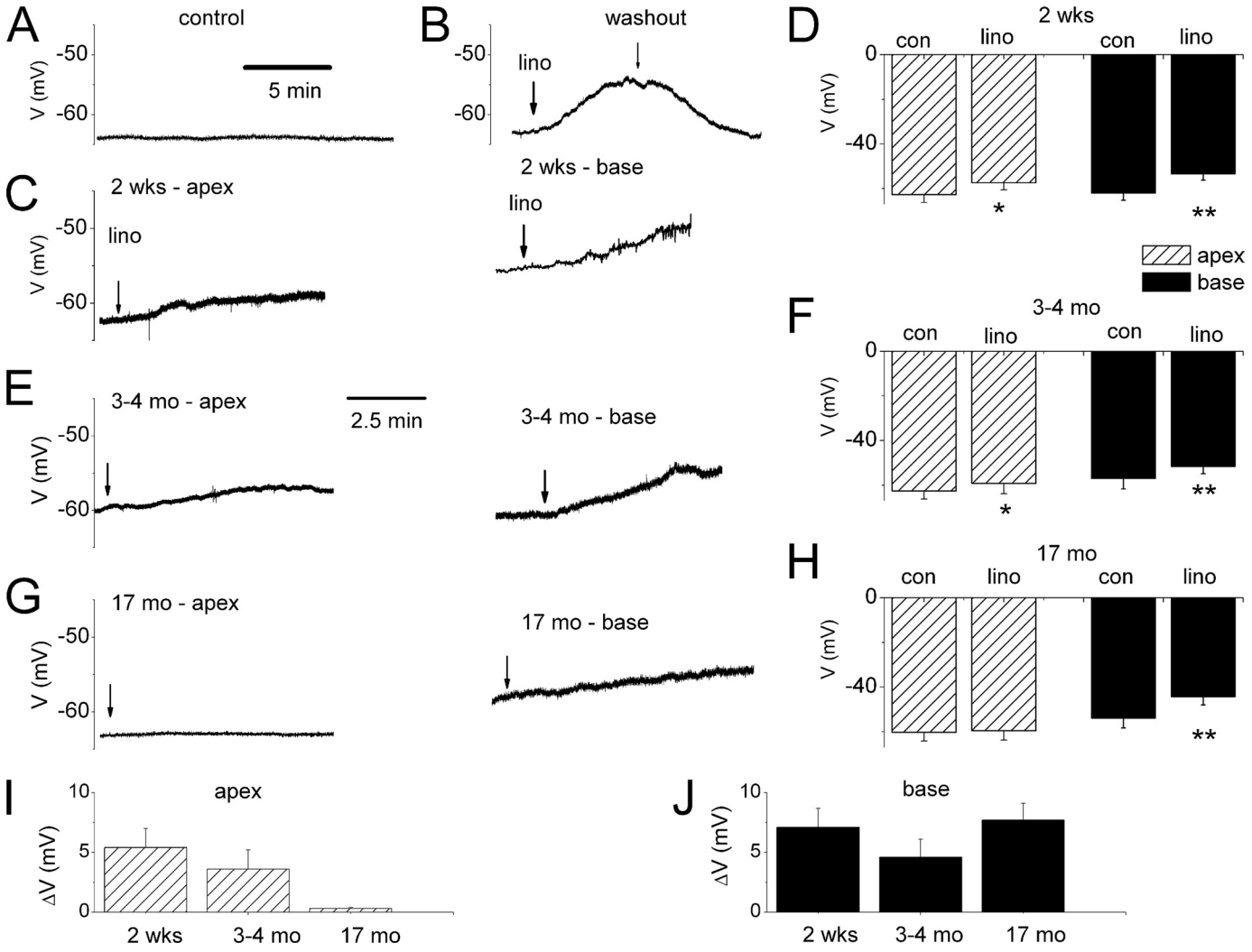

FIGURE 2. **Effects of blockage of K_v7 currents on the resting membrane potential (V_{rest}).** *A*, shown is characteristic V_{rest} of a 0.5-month-old apical SGN under control conditions. *B*, application of linopirdine (*lino*, 10 μM)-induced membrane depolarization in basal 0.5-month-old basal SGN (*upper panel*). The effect of the drug was reversible after washout. *C* depicts the effect of linopirdine on 0.5-month-old (*mo*) (2 week (*wk*)) apical (*left panel*) and basal (*right panel*). *D*, summary data of changes in V_{rest} in apical and basal SGNs of 0.5-month-old mice ($n = 11$; *, $p < 0.05$; **, $p < 0.01$). *con*, control. *E*, examples of raw traces showing changes in V_{rest} after application of linopirdine in apical (*left panel*) and basal SGNs isolated from 3- to 4-month-old mice. *F*, corresponding summary data obtained from 3- to 4-month-old SGNs ($n = 7$). *G*, linopirdine had very little effect on apical neurons isolated from 17-month-old mice compared with age-matched basal SGNs. *H*, summary data of the effects linopirdine on V_{rest} of apical and basal 17-month-old neurons. *I* and *J* show changes in V_{rest} in different aged group of neurons at apical (*I*) and basal (*J*) aspects of the cochlea.

final concentration of DMSO in the recording bath solution was ~0.001%.

Measurement of Relative Levels of Cytoplasmic Ca^{2+}—We recorded the relative levels of intracellular Ca^{2+} concentrations from SGNs. A fluorometric method with Fluo-4/AM as the Ca^{2+} indicator was used for assessing the relative cytoplasmic Ca^{2+} concentrations. SGNs were incubated in external solution with 1 μM Fluo-4/AM and pluronic F-127 (0.1%) for 15 min at room temperature. Linopirdine, retigabine, and high external K^+ concentrations (10 mM) were added to the perfusate, and the Ca^{2+}-dependent fluorescence was measured. Using a Zeiss LSM510 meta confocal microscope, excitation of Fluo-4 was performed with an argon laser at 488 nm, and the emitted light was reflected through a 505–550-nm bandpass filter from a 540-nm dichroic mirror. Data were captured with LSM510 software (Zeiss).

Terminal dUTP Nick-end Labeling (TUNEL) Assay—SGNs under different treatment conditions were fixed in 4% paraformaldehyde for 20 min. After three washes in PBS, SGNs were postfixed in ethanol/acetic acid (2:1) for 5 min. Following two washes in PBS, a 50-μl TUNEL reaction mixture (*in situ* cell death detection-fluorescein, Roche Applied Science) was added and incubated in the dark and humidified chamber for ~2 h at 37 °C. The specimens were washed three times in PBS and were counterstained with 4′,6-diamidino-2-phenylindole·2HCl (DAPI), mounted, and viewed under a LSM510 confocal microscope.

RESULTS

Properties of K_v7 Channel Currents in SGNs and Alteration during Aging—To assess K_v7 channel currents expressed by SGNs functionally, we capitalized on the sensitivity of the currents to linopirdine (9, 20). We applied 10 μM linopirdine after recording the whole-cell outward K^+ currents. Inward currents were suppressed by replacing external Na^+ and Ca^{2+} with choline and Mg^{2+}. Fig. 1, *A* and *B*, shows outward K^+ currents

recorded from mice 0.5-month (2 weeks)- and 17-month-old SGNs, isolated from the apex of the cochlea, before and after application of linopirdine. The linopirdine-sensitive (difference) current traces are shown below Fig. 1, *A* and *B*. Similarly, we examined the whole-cell K^+ currents from SGNs from the base of the cochlea and compared the current magnitudes between 0.5- and 17-month-old neurons (Fig. 1, *C* and *D*). The linopirdine-sensitive currents, denoted henceforth as K_v7-mediated current, are shown below the original traces. The total K^+ current magnitude varied between apical and basal SGNs, and the expression of the current differed during aging. For example, at a 0-mV step potential, the magnitude of the whole-cell K^+ currents at the base were (base; in pA/picofarad) as follows: 0.5 month, 112 ± 18; 3–4 month, 78 ± 10; and 17 month, 111 ± 8 (n = 17). On the other hand, the magnitude of apical whole-cell K^+ currents was invariably smaller than current from basal SGNs (apex; in pA/picofarad) as follows: 0.5 month, 81 ± 7; 3–4 month, 73 ± 11; and 17 month, 101 ± 5 (n = 17). Meanwhile, the contribution of K_v7-mediated currents in apical SGNs (Fig. 1*E*) was modest and varied from 12% at 0.5 month, 10% at 3–4 month, and 17% at 17 month. By contrast, the K_v7-mediated current in basal SGNs (Fig. 1*F*) constituted a substantial portion of the whole-cell K^+ current ranging from 21% at 0.5 month, 15% at 3–4 months, and 26% at 17 months. Analyses of the tail currents showed that the voltage-dependent activation of K_v7-mediated currents showed a tendency for basal cells to be activated at a more negative voltage, with $V_{½}$ = −48 ± 3 mV and slope factor, k, of 18 ± 4 mV (n = 17) compared with apical cells with $V_{½}$ = −45 ± 5 mV and k = 20 ± 3 mV (n = 16). Moreover, there were no significant changes in the voltage-dependent properties of the current during aging (Fig. 1*G*, legend).

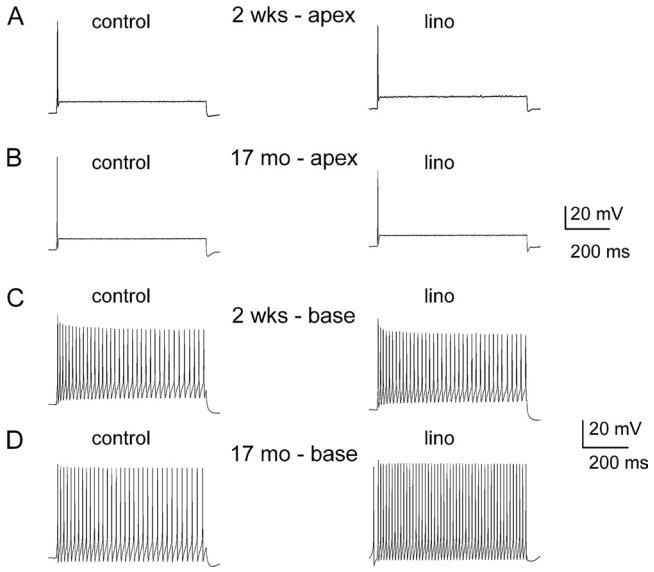

FIGURE 3. **Effects of blockage of K_v7 currents on membrane excitability of SGNs.** *A,* injection of 0.1 nA current produced single spikes in apical SGNs isolated from 2-week-old (0.5-month) mice. We denoted these neurons as rapidly adapting neurons. Linopirdine (*lino*) had no noticeable effect on spike activity. *B,* similar data were obtained from 17-month-old apical SGNs. The summary data are outlined in Table 1 (also see supplemental Tables). *C* and *D,* in contrast, injection of 0.1 nA current produced multiple spikes in basal neurons (denoted as slowly adapting neurons), which was further enhanced upon application of linopirdine. *C* depicts recordings from 2-week-old mice and *D* represents data from 17-month-old SGNs. Summary data of the effects of linopirdine on the number of spikes are shown in Table 1.

Effects of Blocker and Enhancer of K_v7 Channel Currents on Membrane Properties of SGNs—Because substantial portions of the K_v7-mediated current are activated at potentials close to V_{rest} of SGNs (−70 to −50 mV), and because of the differential expression of the current along the axis of the cochlea and during development, we examined the effects of linopirdine on the membrane properties of SGNs. The V_{rest} of SGNs was invariably stable under control conditions as shown for an apical neuron from a 0.5-month-old mouse (Fig. 2*A*). Linopirdine produces reversible depolarization of the V_{rest} of SGNs (Fig. 2*B*). For 0.5-month-old SGNs, depolarization of V_{rest} was most prominent in basal neurons ($p < 0.01$) compared with apical ones (Fig. 2, *C* and *D*). Similarly, linopirdine-induced alterations of V_{rest} were documented in 3–4 month-old neurons (Fig. 2*E* and summary data in Fig. 2*F*, $p < 0.05$). By contrast, by 17 months, the effects of linopirdine were statistically unchanged in apical neurons compared with basal cells (Fig. 2, *G* and *H*, $p < 0.05$). The summary data on linopirdine-mediated changes in membrane potentials are shown in Fig. 2, *I* and *J*. Next, we examined the ensuing outcome of the effects of linopirdine on the firing pattern and frequency of action potentials (APs) in SGNs. Besides depolarization of V_{rest}, no changes in the evoked AP profile or frequency were observed in apical neurons at all ages (Fig. 3, *A* and *B*, and supplemental Tables S1 and S2). Other marked differences seen in the aging SGNs were as follows: AP duration, spike frequency, latency, and spike width in basal neurons (supplemental Tables S1 and S2). On the other hand, effects of the K_v7 current blocker on basal neurons

TABLE 1
Effects of linopirdine on membrane properties apical and basal SGNs
Rmp is resting membrane potential.

	Age	Base		Apex		
		Control	Linopirdine		Control	Linopirdine
Spike number	2 weeks (n = 11)	40 ± 13	47 ± 6	n = 12	1 ± 0	1 ± 0
	3–4 months (n = 9)	19 ± 5	40 ± 7[a]	n = 8	1 ± 0	1 ± 0
	17 months (n = 5)	22 ± 7	38 ± 7	n = 6	1 ± 0	1 ± 0
Rmp (mV)	2 weeks (n = 11)	−62 ± 3	−53 ± 3[b]	n = 12	−63 ± 4	−57 ± 3
	3–4 months (n = 9)	−57 ± 4	−51 ± 3[b]	n = 8	−63 ± 4	−60 ± 4
	17 months (n = 5)	−54 ± 4	−44 ± 4[b]	n = 6	−60 ± 4	−60 ± 4
AP duration (ms)	2 weeks (n = 11)	7 ± 1	6 ± 1	n = 12	9 ± 2	7 ± 1
	3–4 months (n = 9)	8 ± 2	7 ± 2	n = 8	6 ± 1	6 ± 1
	17 months (n = 5)	7 ± 0	6 ± 2	n = 6	6 ± 1	6 ± 1

[a] $p < 0.01$ treatment *versus* control.
[b] $p < 0.05$.

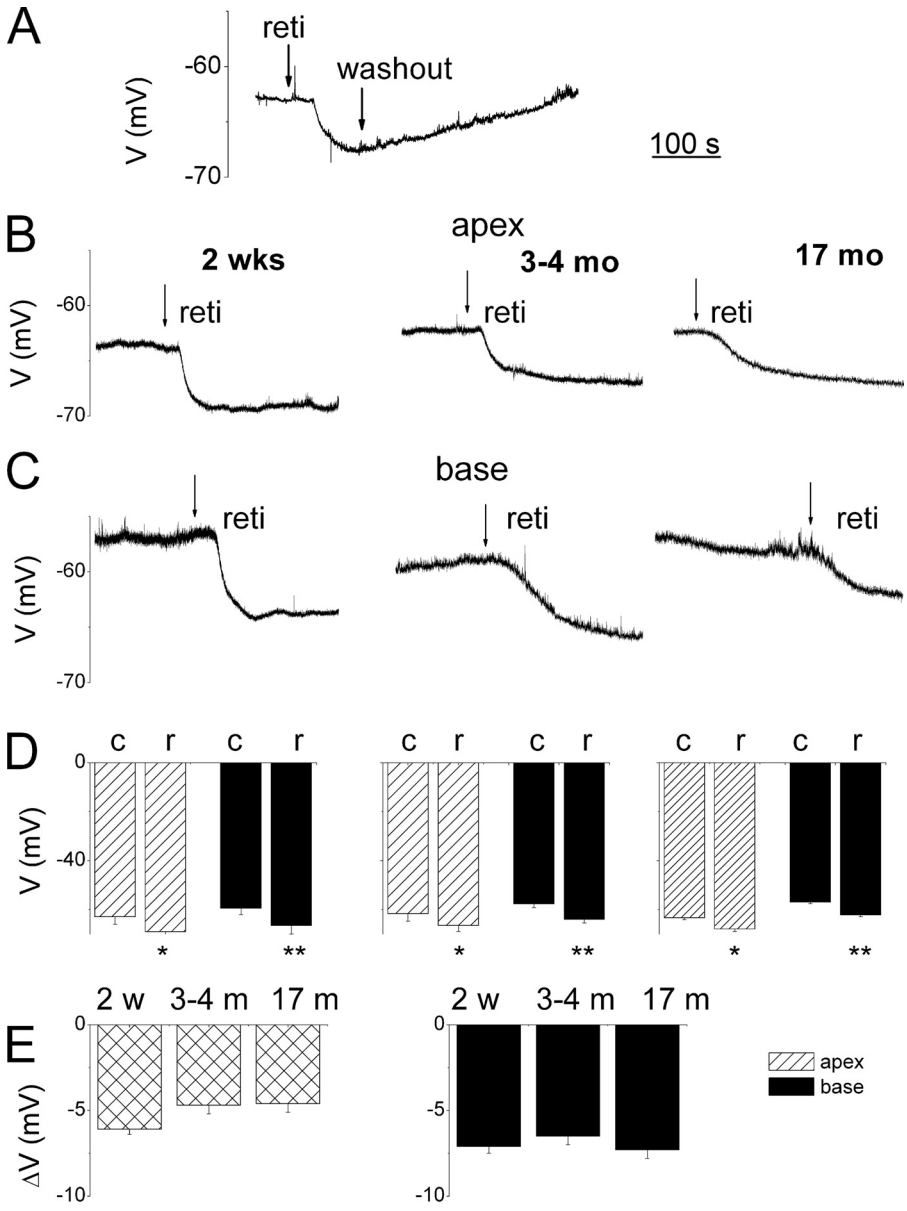

FIGURE 4. **Retigabine-mediated membrane hyperpolarization in SGNs.** *A,* typical recordings of the V_{rest} of SGN. Application of 10 μM retigabine (*reti* or *r*), K_v7 channel opener, resulted in reversible hyperpolarization of V_{rest}. *B,* exemplary recordings from 2-week-old (0.5-month, *left panel*) and, 3–4-month-old (*middle panel*) and 17-month-old (*right panel*) SGNs isolated from apical aspects of the cochlea. *C,* similarly, basal SGNs also underwent changes in V_{rest}. Shown are depictions of data from 2-week-old (0.5-month-old. *left panel*), 3–4-month-old (*middle panel*), and 17-month-old (*right panel*) basal SGNs. *D,* summary data illustrated in the form of *histograms*. Data from 2-week-old (0.5 months, $n = 15$, *left panel*) and 3–4-month-old ($n = 14$; *middle panel*) and 17-month-old ($n = 11$; *right panel*), where *solid rectangles* represent basal and *striped rectangles* represent apical SGNs. (*c,* control; *r,* retigabine; *, $p < 0.05$; **, $p < 0.01$ l *w*, week; *m*, month.) *E,* summary data tabulated for the changes in V_{rest} after application of retigabine for different aged groups: *2 w* = 2 weeks; $n = 11$; 3–4-month-old ($n = 12$) and 17-month-old ($n = 10$) apical (*left panel*) and basal (*right panel*) neurons (see Table 2 and supplemental tables).

were seen mainly as increased AP frequency (Fig. 3, *C* and *D*, Table 1, and supplemental Tables S3–S5).

To ensure that linopirdine-mediated alterations of V_{rest} and evoked APs were K_v7 current-specific, we examined the effects of a K_v7 channel opener, retigabine, on the membrane properties of SGNs. Consistent with the presence of K_v7 currents in SGNs, retigabine (10 μM) produced reversible hyperpolarization of the membrane potential (Fig. 4*A*). Apical and basal SGNs at 0.5, 3–4, and 17 months old responded equally to retigabine, resulting in significant hyperpolarization of the membrane potentials (Fig. 4, *B–E*). Consequently, there were corresponding reductions in the excitability of neurons producing robust reduction in spike numbers elicited in basal SGNs (Fig. 5 and Table 2). The effects of retigabine could be seen in SGNs at all ages examined (0.5–17 months old), suggesting the K_v7-mediated currents remain prominent in the life span of the neurons. Moreover, the effects of the drug on basal neurons were more pronounced than apical neurons (Table 2; also see supplemental Table S6–S8).

Altered Conductance of K_v7 Channel Currents Results in Changes in Intracellular Ca^{2+}—The voltage ranges at which K_v7-mediated currents appear to predominate are relatively low (negative), and SGNs have been reported to express not only transient but also sustained low voltage-activated Ca^{2+} currents (21–25). Accordingly, we predicted that linopirdine would invoke membrane depolarization, which will promote Ca^{2+} influx through activation of voltage-gated Ca^{2+} channels to increase intracellular Ca^{2+}. Retigabine would be expected to produce an opposite effect. We measured intracellular Ca^{2+} changes using Fluo-4 fluorescence in the absence and presence of linopirdine (Fig. 6*A*). To examine the effects of retigabine on intracellular Ca^{2+}, we depolarized SGNs by increasing the external K^+ concentration from 2 to 10 mM, which was sufficient to produce an ~30-mV change in membrane voltage, producing an increase in intracellular Ca^{2+} (Fig. 6*B*). Perfusion of retigabine resulted in gradual reduction of intracellular Ca^{2+}, findings that are in keeping with the drug-mediated changes in the membrane potential of SGNs.

Blockage of K_v7-mediated Currents Results in Apoptotic SGN Death—It has been demonstrated that membrane depolarization and Ca^{2+} influx through voltage-gated Ca^{2+} channels promote SGN survival *in vitro* (13). Also important, and of significant clinical implications *in vivo*, is the finding that direct electrical stimulation of SGNs via an implanted electrode may

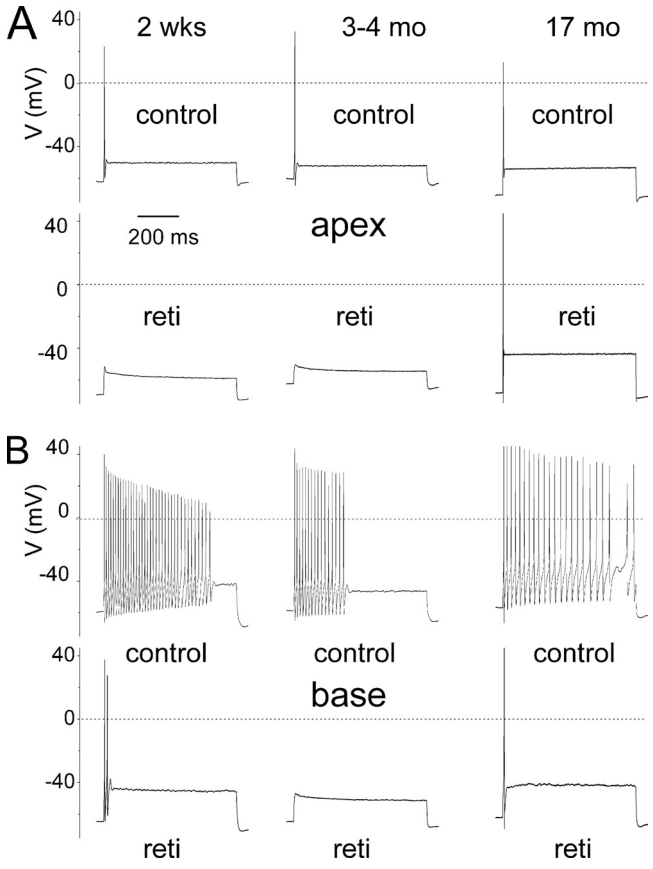

FIGURE 5. **Retigabine, a K_v7-mediated current agonist, attenuated the excitability of SGNs from the apical and basal turn of the cochlea.** *A,* action potentials were recorded from SGNs isolated from the apical turn of the cochlea by current injection of 0.1 nA. Shown are representative profiles recorded from 2-week-old (*left panel*) and 3–4- and 17-month-old SGNs. *B,* using similar recordings from basal SGNs, control neurons responded to current (0.2 nA) injected with repetitive firing that showed adaptation. Retigabine (*reti*) (10 μM) attenuated the AP firing. The number of spikes elicited and V_{rest} in apical cells for control were 1 ± 0 and −66 ± 4 mV and after application of retigabine were 0 ± 0 ($n = 9$) and −75 ± 5 mV, respectively. The number of spikes elicited and V_{rest} in basal cells for control were 29 ± 12 and −59 ± 3 mV and after application of retigabine were 1.5 ± 0.7 ($n = 9$) and −66 ± 3 mV, respectively.

increase SGN survival after hair cell loss (26). We examined the effects of long term blockage of K_v7-mediated currents *in vitro* on SGNs (~48 h) using TUNEL assay to determine neuronal survival under different control conditions as follows: 1) no growth factors; 2) in the presence of brain-derived neurotrophic factor (BDNF) and neurotrophin-3 (NT3); 3) at high extracellular K^+ (10 mM) to induce sustained depolarization and by deduction an unrelenting increase in intracellular Ca^{2+}; 4) inhibition of K_v7-mediated current by linopirdine; and 5) the apoptosis-induced drug 7,12-dimethylbenz[*a*]anthracene as a positive control (Fig. 7, *A* and *B*). SGNs in culture showing positive reactivity in TUNEL assay were counted and normalized against the total number of neurons as determined by TUJ1 neuronal marker reaction. The summary data shown in the *histogram* in Fig. 7*B* demonstrated that exposure of neurons in culture to 10 μM linopirdine resulted in a significant increase in apoptotic cell death ($p < 0.01$) compared with conditions of no growth factors and with BDNF and NT3. Indeed, the effect of linopirdine was equivalent to high K^+ (10 mM)-induced depolarization of SGNs. In keeping with the functional data, the effects of linopirdine were pronounced in basal compared with apical neurons. Finally, we assessed the effects of linopirdine on apical and basal neurons (Fig. 8*A*) under reduced extracellular Ca^{2+} concentrations ($[Ca^{2+}]$). To do this, we added EGTA in the culture media to obtain a final estimated $[Ca^{2+}]$ of ~300 μM. Additionally, we reduced Ca^{2+} influx through voltage-gated Ca^{2+} channels by blocking a variety of Ca^{2+} currents (Fig. 8*B,* also see supplemental Fig. S1). By reducing Ca^{2+} entry, the effects of linopirdine on basal neurons were significantly reduced. Thus, Ca^{2+}-mediated neuronal benefits (13) may require tightly regulated mechanisms to finely tune the survival and death pathways. SGN depolarization that may ensue from reduced and removed activity of K_v7-mediated currents may ultimately result in neuronal degeneration as seen in DFNA2.

DISCUSSION

Several important issues remain unresolved regarding the etiology and mechanism by which mutations in $K_v7.4$ result in progressive hearing loss associated with degeneration of hair cells and SGNs, which is manifested as high-to-low frequency hearing loss (4–7, 9, 10, 20). Previous studies have suggested that in the inner ear the $K_v7.4$ channel is highly expressed in IHC and outer hair cells (4). Because K_v7 channel-mediated currents are activated at low membrane voltages, it has been suggested and demonstrated that $K_v7.4$ currents contribute substantially in establishing V_{rest} of IHCs and, in so doing, control intracellular Ca^{2+} concentrations (15, 16). Although not demonstrated either *in vitro* or *in vivo*, the implications of these findings are that a pathological rise in intracellular Ca^{2+} may ensue due to reduced expression or dysfunction of $K_v7.4$ in DFNA2, leading to cell death. In contrast, no information exists regarding the functional roles of K_v7 channel currents in SGNs and whether degeneration of neurons in DFNA2 can be explained from primary alterations of channel functions or secondary consequences of hair cell loss through target-deprived neuronal degeneration. Moreover, a critical issue that had not been addressed fully was whether $K_v7.2$–3/5 was also expressed in SGNs. The ramifications of expression of other subtypes of K_v7 channels could be vast, because α-subunits of $K_v7.2$–5 undergo promiscuous association to form tetrameric channels (20). Thus, a dominant negative version of $K_v7.4$ can potentially cripple K_v7-mediated current in SGNs. Recently, it has been demonstrated that SGNs do express a variety of K_v7 channels, raising the possibility of a more complex cellular mechanism for DFNA2 (14).

In this study, we have identified a base-to-apex gradient of K_v7 currents in SGNs, defined by their sensitivity to linopirdine and retigabine. It is unclear why the action of linopirdine appeared slower than retigabine. The presence of K_v7 currents in SGNs is consistent with the immunolocalization of K_v7 channels reported previously and recently (7, 14, 27). Also important, we demonstrated that differential expression of K_v7 currents results in distinct and profound variations of the membrane properties of basal *versus* apical SGNs following blockage of the current. Although linopirdine had little effect on apical SGNs, the drug had profound excitatory effects on basal SGNs. As expected, retigabine, a K_v7 channel opener, attenuated AP

TABLE 2
Effects of retigabine on membrane properties of SGNs
Rmp is resting membrane potential.

	Age	Base		Apex		
		Control	Retigabine		Control	Retigabine
Spike number	2 weeks ($n = 4$)	29 ± 12	2 ± 1	$n = 5$	1 ± 0	0[a]
	3–4 months ($n = 7$)	20 ± 6	0.4 ± 0.5[a]	$n = 8$	1 ± 0	0[a]
	17 months ($n = 5$)	22 ± 6	1 ± 1[a]	$n = 6$	1 ± 0	0[a]
Rmp (mV)	2 weeks ($n = 4$)	−58 ± 2	−64 ± 1[b]	$n = 5$	−66 ± 4	−75 ± 5[b]
	3–4 months ($n = 7$)	−59 ± 3	−66 ± 3[b]	$n = 8$	−62 ± 2	−66 ± 3
	17 months ($n = 5$)	−59 ± 3	−69 ± 2[a]	$n = 6$	−61 ± 2	−67 ± 2[b]
AP duration (ms)	2 weeks ($n = 4$)	7 ± 1		$n = 4$	6 ± 2	
	3–4 months ($n = 7$)	8 ± 2		$n = 7$	8 ± 1	
	17 months ($n = 5$)	6 ± 2	3 ± 0[a]	$n = 6$	7 ± 1	

[a] $p < 0.01$ treatment *versus* control.
[b] $p < 0.05$.

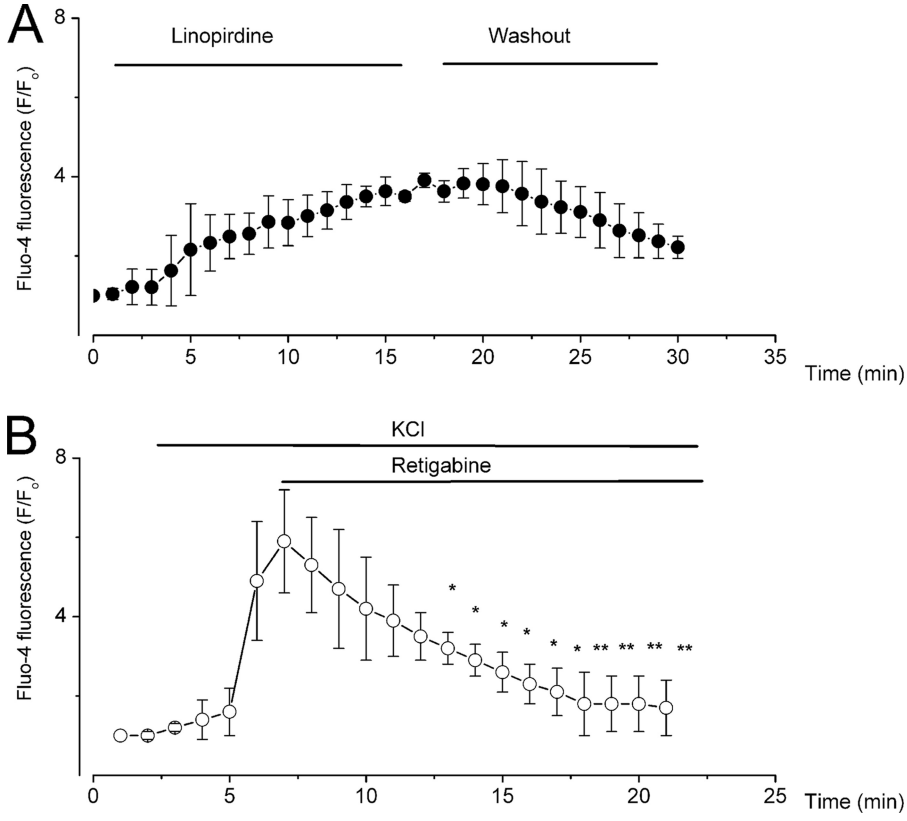

FIGURE 6. **Changes in $Ca^{2+}{}_i$ after blockade and enhancement of K_v7-mediated current by linopirdine and retigabine, respectively.** SGNs were loaded with Fluo 4/AM, and the changes in $[Ca^{2+}]_i$ were monitored by measuring the fluorescence intensity. *A,* effects of 10 μM linopirdine showing a steady and sustained rise in $[Ca^{2+}]_i$. Shown is the effect of linopirdine and partial recovery after washout of the drug. *B,* to determine the effects of retigabine, we depolarized Fluo 4-loaded SGNs with 10 mM KCl before application of 10 μM retigabine in 10 mM KCl solution. Retigabine reversed the effects of high external K^+ by reducing $[Ca^{2+}]_i$. Summary data were obtained from $n = 5$ (*, $p < 0.5$; **, $p < 0.01$).

induced by current injection. If inhibitors of K_v7 currents produce a major impact on the V_{rest} of SGNs, as demonstrated by the excitatory effect of linopirdine and inhibitory actions of retigabine, then we predicted that linopirdine would mediate an increase in Ca^{2+} influx through activation of voltage-gated Ca^{2+} currents. Linopirdine did not have any effect on Ca^{2+} currents in SGNs (data not shown). However, inhibition of K_v7-mediated current resulted in a sustained increase in intracellular Ca^{2+} and activation of K_v7 channels produced the opposite effects. It can be inferred that linopirdine blocked K_v7-mediated currents to promote membrane depolarization, which in turn activated Ca^{2+} currents to increase Ca^{2+} influx. Moreover, other potential sources of Ca^{2+} cannot be ruled out completely because the mixture of Ca^{2+} channel blockers and reduced external Ca^{2+} did not reverse the effects of linopirdine entirely to control levels (see Figs. 7*B* and 8*B*). It can also be argued that Ca^{2+} influx through voltage-gated Ca^{2+} channels is the main source of Ca^{2+}, because the dosage of Ca^{2+} channel blockers used was not saturating, and modest Ca^{2+} influx was expected to persist under reduced external Ca^{2+} concentration (~300 μM). Paradoxically, it has been demonstrated that membrane depolarization and Ca^{2+} influx through voltage-dependent Ca^{2+} channels promote SGN survival *in vitro* (13, 28). Thus, in contrast to IHCs, where Ca^{2+} has been inferred to mediate cell degeneration, it was predicted to mediate distinct pro-survival signaling in SGNs (28).

Surprisingly, in contrast to previous assertions, we have demonstrated that a sustained increase in intracellular Ca^{2+} mediated by linopirdine resulted in significant SGN apoptotic death. Indeed, the effect of linopirdine plummeted significantly by reduced extracellular Ca^{2+} and by application of Ca^{2+} channel blockers in basal SGNs. However, the results are in keeping with a recent report demonstrating that SGN membrane depolarization may inhibit neurite outgrowth by way of activation of multiple voltage-dependent Ca^{2+} channels and calpain (25). Our results imply that although a moderate rise in intracellular Ca^{2+} may mediate activation of factors that promote neurite outgrowth and survival, a sustained increase in Ca^{2+} may result in Ca^{2+}-dependent cell death (29–32). Besides revealing traces of the cellular mechanisms of SGN degeneration, these findings also divulge the importance of understanding the finely tuned mechanisms

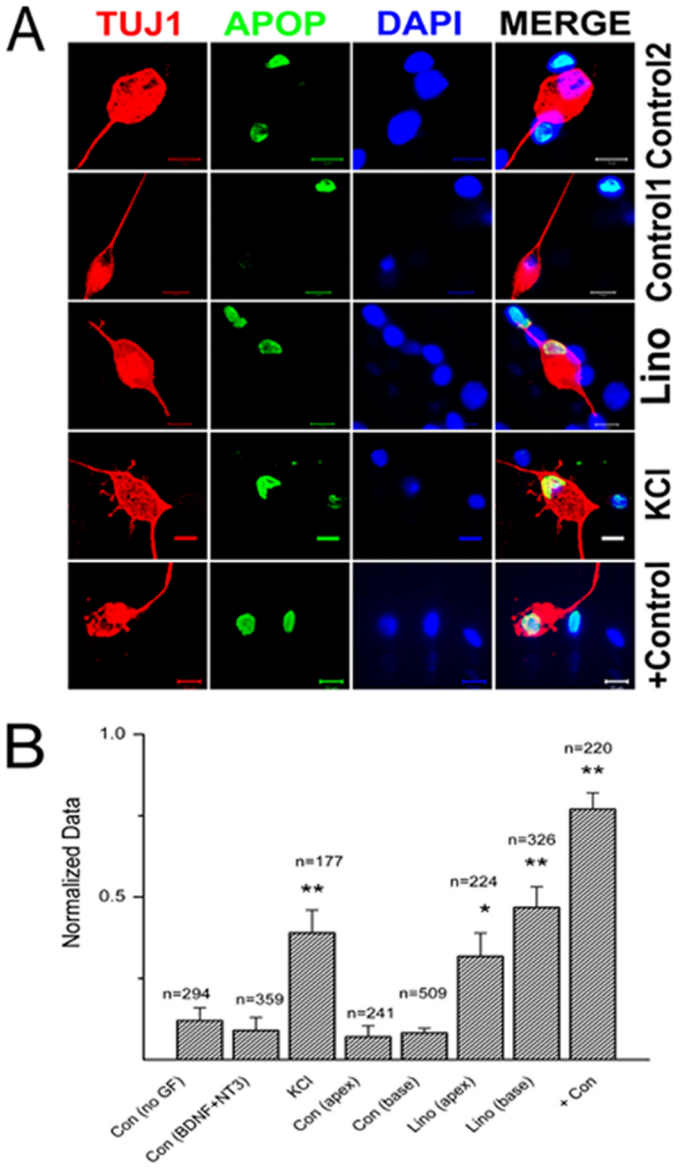

FIGURE 7. **Qualitative assessment of SGNs apoptosis.** *A, upper panel* shows SGNs in *control*(*2*) culture with BDNF/NT3 growth factors. Note that there are non-neuronal cells undergoing apoptosis, but invariably, most of the SGNs were intact. The *2nd upper panel* is from *control*(*1*) culture with no growth factors (*GF*). The number of apoptotic SGNs increased when cultures were treated with 10 μM linopirdine (*lino*, *3rd row*) and 10 mM KCl for 72 h. The *bottom row* serves as a positive control (*Con*) with treatment of 1 μM 12-dimethylbenz[*a*]anthracene. *TUJ1*, neuronal marker; *Apop* (apoptosis = TUNEL-positive; *DAPI* = nuclei stain). *B,* quantitative assessment of SGNs apoptosis histograms, comparing the ratio of TUNEL-positive SGNs under different experimental conditions. Control 1, have no growth factor; control 2, contained BDNF/NT3, 10 mM, KCl, 10 μM linopirdine (*lino*), comparison of baseline data for apical and basal SGNs with linopirdine-treated conditions, and finally, after application of positive control = 1 μM 12-dimethylbenz[*a*]anthracene. **, $p < 0.01$.

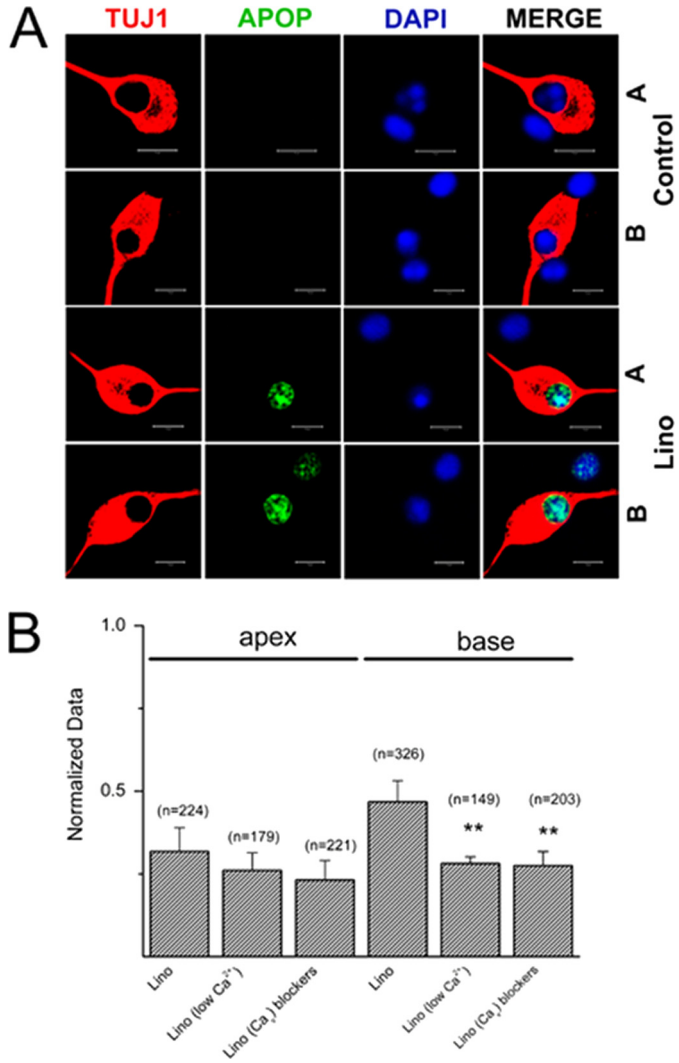

FIGURE 8. **Analyses of the effects of linopirdine under reduced extracellular Ca^{2+} conditions and assessment of SGNs apoptosis.** *A, upper panel* shows SGNs in control culture with BDNF/NT3 growth factors. *A* denotes apical and *B* denotes basal SGNs. Consistent with the data in Fig. 7, the number of apoptotic SGNs increased when cultures were treated with 10 μM linopirdine (*lino, 3rd* and *4th rows*) for 72 h. *TUJ1*, neuronal marker; *Apop* (apoptosis = TUNEL-positive; DAPI = nuclei stain). *B,* quantitative assessment of SGNs apoptosis histograms, comparing the relative number of TUNEL-positive SGNs under different experimental conditions. 10 μM *lino* = linopirdine, comparison of base-line data for apical and basal SGNs with linopirdine-treated conditions. Low bath Ca^{2+} concentration of ~300 μM was achieved by adding 2 mM EGTA to the culture media. We reduced Ca^{2+} currents using a mixture of Ca^{2+} channel (Ca_v) blockers; 1 μM mibefradil to block T-type, rSNX-482 for R-type, 1 μM ω-conotoxin GVIA for N-type, 1 μM ω-agatoxin IVA for P/Q-type, and 10 μM nimodipine for L-type Ca^{2+} currents. Reduction of Ca^{2+} influx by decreasing bath Ca^{2+} or blocking Ca_v significantly reduced the effects of linopirdine. **, $p < 0.01$.

of Ca^{2+} handling in SGNs. Also important, and of significant implications *in vivo*, is the finding that direct electrical stimulation of SGNs via an implanted electrode may increase SGN survival after hair cell loss (26, 33), prompting the need to adopt stimulation paradigms that will promote optimal SGN survival without inducing cell death.

Mechanistic Implication of DFNA2—Several plausible mechanisms can be conceived to explain mutations at multiple sites in $K_v7.4$ channels that result in SGN degeneration associated with DFNA2 (9). One model will assert that because the expression pattern of several K^+ channels, such as $K_v4.2$, $K_v1.1$, $K_v3.1$, and Ca^{2+}-dependent K^+ channels in SGNs, show distinct apico-basal gradient (34–37), and in DFNA2 the brunt of reduced activity of $K_v7.4$ is manifested first in basal neurons. Consequently, increased membrane depolarization ensues, followed by sustained Ca^{2+} influx through voltage-gated Ca^{2+} channels resulting in Ca^{2+}-induced cell death. Subsequently, because of generalized age-related changes in the expression of

$K_v1.1$ and $K_v3.1$ in cochlear neurons (38), apical SGNs are impacted. Another model may ascribe the phenotype in DFNA2 primarily to hair cell degeneration (39), although this is unlikely because SGNs appear to express similar levels of $K_v7.4$ channels (6, 7). Nonetheless, SGN degeneration is attributed to the initial loss of hair cells. The activity of hair cells and their trophic inputs to SGNs are important for their survival (12, 40). Thus, the initial irreversible damage of cochlear hair cells leads to degeneration of target-deprived SGNs.

Alternatively, these models may not be mutually exclusive. Moreover, in both cases our finding that $K_v7.4$ and $K_v7.2–5$ undergo indiscriminate interactions to form tetrameric channels presents a quandary that has diverse functional and severe pathological ramifications (20). Although K_v7 heterotetrameric channels may produce wide ranging diversity in functional properties of the ensuing currents, the expression of a dominant negative mutant of $K_v7.4$ can potentially cripple the functions of the entire family of K_v7 subunits (20) in SGNs. Furthermore, determination of the properties of native K_v7 channels may be obscured by regulation of KCNE subunits (41) and the α-subunit interaction with $K_v10.1$ (ERG1) (42–44). Thus, null deletion of one subtype of K_v7 channels may produce a modest phenotype (39), but a dominant negative version of a $K_v7.4$ channel subunit will impair the entire K^+ channel class, resulting in a profound auditory phenotype (16, 20).

Acknowledgments—We thank Dr. N. Chiamvimonvat and members of our laboratory for their constructive comments. Retigabine was provided by Dr. Michael A Rogawski, University of California, Davis.

REFERENCES

1. Howard, R. J., Clark, K. A., Holton, J. M., and Minor, D. L., Jr. (2007) *Neuron* **53,** 663–675
2. Chung, H. J., Jan, Y. N., and Jan, L. Y. (2006) *Proc. Natl. Acad. Sci. U.S.A.* **103,** 8870–8875
3. Hübner, C. A., and Jentsch, T. J. (2002) *Hum. Mol. Genet.* **11,** 2435–2445
4. Kharkovets, T., Hardelin, J. P., Safieddine, S., Schweizer, M., El-Amraoui, A., Petit, C., and Jentsch, T. J. (2000) *Proc. Natl. Acad. Sci. U.S.A.* **97,** 4333–4338
5. Kubisch, C., Schroeder, B. C., Friedrich, T., Lütjohann, B., El-Amraoui, A., Marlin, S., Petit, C., and Jentsch, T. J. (1999) *Cell* **96,** 437–446
6. Beisel, K. W., Nelson, N. C., Delimont, D. C., and Fritzsch, B. (2000) *Brain Res. Mol. Brain Res.* **82,** 137–149
7. Beisel, K. W., Rocha-Sanchez, S. M., Morris, K. A., Nie, L., Feng, F., Kachar, B., Yamoah, E. N., and Fritzsch, B. (2005) *J. Neurosci.* **25,** 9285–9293
8. Hurley, K. M., Gaboyard, S., Zhong, M., Price, S. D., Wooltorton, J. R., Lysakowski, A., and Eatock, R. A. (2006) *J. Neurosci.* **26,** 10253–10269
9. Jentsch, T. J. (2000) *Nat. Rev. Neurosci.* **1,** 21–30
10. Seal, R. P., Akil, O., Yi, E., Weber, C. M., Grant, L., Yoo, J., Clause, A., Kandler, K., Noebels, J. L., Glowatzki, E., Lustig, L. R., and Edwards, R. H. (2008) *Neuron* **57,** 263–275
11. Martinez-Monedero, R., Corrales, C. E., Cuajungco, M. P., Heller, S., and Edge, A. S. (2006) *J. Neurobiol.* **66,** 319–331
12. Eatock, R. A., and Hurley, K. M. (2003) *Curr. Top. Dev. Biol.* **57,** 389–448
13. Hegarty, J. L., Kay, A. R., and Green, S. H. (1997) *J. Neurosci.* **17,** 1959–1970
14. Jin, Z., Liang, G. H., Cooper, E. C., and Jarlebark, L. (2009) *Audiol. Neurootol.* **14,** 98–105
15. Oliver, D., Knipper, M., Derst, C., and Fakler, B. (2003) *J. Neurosci.* **23,** 2141–2149
16. Holt, J. R., Stauffer, E. A., Abraham, D., and Géléoc, G. S. (2007) *J. Neurosci.* **27,** 8940–8951
17. Wei, D., Jin, Z., Järlebark, L., Scarfone, E., and Ulfendahl, M. (2007) *Dev. Neurobiol.* **67,** 108–122
18. Levic, S., Nie, L., Tuteja, D., Harvey, M., Sokolowski, B. H., and Yamoah, E. N. (2007) *Proc. Natl. Acad. Sci. U.S.A.* **104,** 19108–19113
19. Rodriguez-Contreras, A., and Yamoah, E. N. (2001) *J. Physiol.* **534,** 669–689
20. Xu, T., Nie, L., Zhang, Y., Mo, J., Feng, W., Wei, D., Petrov, E., Calisto, L. E., Kachar, B., Beisel, K. W., Vazquez, A. E., and Yamoah, E. N. (2007) *J. Biol. Chem.* **282,** 23899–23909
21. Santos-Sacchi, J. (1993) *J. Neurosci.* **13,** 3599–3611
22. Hisashi, K., Nakagawa, T., Yasuda, T., Kimitsuki, T., Komune, S., and Komiyama, S. (1995) *Hear. Res.* **91,** 196–201
23. Wildburger, N. C., Lin-Ye, A., Baird, M. A., Lei, D., and Bao, J. (2009) *Mol. Neurodegener.* **4,** 44
24. Shen, H., Zhang, B., Shin, J. H., Lei, D., Du, Y., Gao, X., Wang, Q., Ohlemiller, K. K., Piccirillo, J., and Bao, J. (2007) *Hear. Res.* **226,** 52–60
25. Roehm, P. C., Xu, N., Woodson, E. A., Green, S. H., and Hansen, M. R. (2008) *Mol. Cell. Neurosci.* **37,** 376–387
26. Leake, P. A., Hradek, G. T., and Snyder, R. L. (1999) *J. Comp. Neurol.* **412,** 543–562
27. Beisel, K. W., Shiraki, T., Morris, K. A., Pompeia, C., Kachar, B., Arakawa, T., Bono, H., Kawai, J., Hayashizaki, Y., and Carninci, P. (2004) *Genomics* **83,** 1012–1023
28. Bok, J., Wang, Q., Huang, J., and Green, S. H. (2007) *Mol. Cell. Neurosci.* **36,** 13–26
29. Semenova, M. M., Mäki-Hokkonen, A. M., Cao, J., Komarovski, V., Forsberg, K. M., Koistinaho, M., Coffey, E. T., and Courtney, M. J. (2007) *Nat. Neurosci.* **10,** 436–443
30. Choi, D. W. (1988) *Trends Neurosci.* **11,** 465–469
31. Zipfel, G. J., Babcock, D. J., Lee, J. M., and Choi, D. W. (2000) *J. Neurotrauma* **17,** 857–869
32. Choi, D. W., Weiss, J. H., Koh, J. Y., Christine, C. W., and Kurth, M. C. (1989) *Ann. N.Y. Acad. Sci.* **568,** 219–224
33. Vollmer, M., Snyder, R. L., Leake, P. A., Beitel, R. E., Moore, C. M., and Rebscher, S. J. (1999) *J. Neurophysiol.* **82,** 2883–2902
34. Adamson, C. L., Reid, M. A., Mo, Z. L., Bowne-English, J., and Davis, R. L. (2002) *J. Comp. Neurol.* **447,** 331–350
35. Jagger, D. J., and Housley, G. D. (2002) *Neuroscience* **109,** 169–182
36. Lin, X., Chen, S., and Tee, D. (1998) *J. Neurophysiol.* **79,** 2503–2512
37. Mo, Z. L., Adamson, C. L., and Davis, R. L. (2002) *J. Physiol.* **542,** 763–778
38. Jung, D. K., Lee, S. Y., Kim, D., Joo, K. M., Cha, C. I., Yang, H. S., Lee, W. B., and Chung, Y. H. (2005) *Neurol. Res.* **27,** 436–440
39. Kharkovets, T., Dedek, K., Maier, H., Schweizer, M., Khimich, D., Nouvian, R., Vardanyan, V., Leuwer, R., Moser, T., and Jentsch, T. J. (2006) *EMBO J.* **25,** 642–652
40. Pirvola, U., Hallböök, F., Xing-Qun, L., Virkkala, J., Saarma, M., and Ylikoski, J. (1997) *J. Neurobiol.* **33,** 1019–1033
41. Ohyama, H., Kajita, H., Omori, K., Takumi, T., Hiramoto, N., Iwasaka, T., and Matsuda, H. (2001) *Pflugers Arch.* **442,** 329–335
42. Abbott, G. W., and Goldstein, S. A. (2002) *FASEB J.* **16,** 390–400
43. Abbott, G. W., Sesti, F., Splawski, I., Buck, M. E., Lehmann, M. H., Timothy, K. W., Keating, M. T., and Goldstein, S. A. (1999) *Cell* **97,** 175–187
44. Nie, L., Gratton, M. A., Mu, K. J., Dinglasan, J. N., Feng, W., and Yamoah, E. N. (2005) *J. Neurosci.* **25,** 8671–8679